Supplementary Information

Visualizing degradation of nerve agent simulants by functionalized Zr-based MOFs: from solution to hydrogels

Hongyan Su, Pengcheng Huang,* Fang-Ying Wu

College of Chemistry, Nanchang University, Nanchang 330031, China

*Corresponding author: pchuang@ncu.edu.cn (P. Huang), Tel: + 86 79183969514, Fax: + 86 79183969514.

Table of Contents

1. Experiment section

Chemicals and reagents. All chemicals were obtained from commercial sources without any purification. Zirconium chloride ($ZrCl_4$) was purchased from Alfa Aesar Chemical Co. Ltd., Tianjin. Terephthalic acid (BDC), 2-amino-terephthalic acid (BDC-NH_2), 2-hydroxyterephthalic acid (BDC-OH), 2, 5-diaminoterephthalic acid (BDC-$(NH_2)_2$), 2, 5-dihydroxyterephthalic acid (BDC-$(OH)_2$), silver nitrate ($AgNO_3$), and tetrabutylammonium hexafluorophosphate ($TBAPF_6$) were obtained from Aladdin Co. Ltd., Shanghai. N, N'-Dimethylformamide (DMF), dimethyl sulfoxide (DMSO), deuterium oxide (D_2O), hydrochloric acid (HCl), acetonitrile (CH_3CN), triethanolamine (TEOA) and methanol (CH_3OH) were bought from Sinopharm Chemical Reagent Co. Ltd. Diethyl chlorophosphate (DCP), dimethyl methylphosphonate (DMMP), and diethyl cyanophosphonate (DCNP) were acquired from Bentu reagent factory, Chengdu. Agarose was purchased from Shanghai Jingchun Technology Co. Ltd. All aqueous solutions were prepared with ultrapure water (18.2 $M\Omega \cdot cm^{-1}$).

Apparatus and measurements. Fluorescence spectra were performed on an F-4600 spectrometer (Hitachi, Japan) equipped with a xenon lamp source and a 1.0 cm quartz cell, and the excitation and emission slit widths were both 5 nm. The photomultiplier tube voltage was 700 V. The interference from the second-order scattering of the excitation wavelength was eliminated by putting a cutoff filter in front of the detector. Fourier transform infrared (FT-IR) spectra were recorded with KBr pellets on a Nicolet 5700 FT-IR Spectrometer (Nicolet, USA). ^{31}P NMR spectroscopy was obtained on a Bruker spectrometer (AVANCE III HD). Scanning electron microscopy (SEM) was carried out with a FEI Quanta200F scanning electron microscope (FEI Company, USA). The solid-state UV-vis measurements were done on the UV2600 spectrophotometer (Shimadzu, Japan) using an internal 110 mm $BaSO_4$ coated integrating sphere. Powder X-ray diffraction (PXRD) patterns were measured on an X-ray diffractometer (Panalytical) utilizing Cu Kα radiation within the 2θ range of 5-50°. X-ray photoelectron spectroscopy (XPS) is performed on ESCALAB250Xi photoelectron spectrometer (Thermo Fisher Scientific, USA).

Electron spin resonance spectra (ESR) were collected by a Bruker A300 spectrometer upon visible-light irradiation under N_2 atmosphere. For ESR measurement, all samples were dispersed in MeCN/TEOA (5/1, v/v) solution, and then transferred into a sample tube. N_2 sorption isotherm measurements were conducted on a Micromeritics ASAP2460 at 77 K. Thermogravimetric analysis was performed on a TGA 5500 instrument with a heating rate of 10 ^{0}C min^{-1} under N_2 atmosphere.

Determination of ionization potentials of four linkers by cyclic voltammetry (CV). CV curves were collected on a Chenhua CHI660E electrochemical workstation, using glassy carbon disks as the working electrode, a Pt wire as the counter electrode, and Ag/0.01 M $AgNO_3$ + 0.1 M $TBAPF_6$ as the reference electrode. $TBAPF_6$ dissolved in DMSO (0.1 M) was used as the supporting electrolyte. The four linkers were dissolved in the electrolyte, and the electrolyte was bubbled with N_2 gas prior to measurements. The ionization potential (I_p), which represents the energy required to lose electrons, can be calculated by the following equation:[S1]

$$I_p = (E'_{ox}+4.71)\ eV$$

where the onset oxidation potential value (E'_{ox}) is relative to Ag^+/Ag reference electrode.

Synthesis of UiO-66 derivatives. Four UiO-66 derivatives were synthesized according to previous procedures with some modifications.[S2] Typically, in a 30 mL reaction flask, $ZrCl_4$ (0.54 mmol, 125 mg), 5 mL DMF and 1 mL HCl was added into the flask and sonicated for 20 min until completely dissolved. The corresponding linker (0.75 mmol) and another 10 mL DMF were then introduced and the mixture was sonicated an additional 20 min before being heated at 80 °C overnight. After cooling to room temperature, the obtained solid was filtered by centrifugation, washed three times with DMF and methanol, and dried at 90 °C under vacuum. Before use, the materials were activated. Briefly, the solids were immersed in a methanol solution overnight, filtered and dried at 90 °C under vacuum for 12 h.

Fluorescence monitoring of DCP degradation using UiO-66 derivatives. In a typical procedure, the aqueous suspension of one UiO-66 derivative (3 mol%, 10 mL, 1 mg mL^{-1}) was prepared in a microcentrifuge tube. After, DCP (28 μL, 19 μmol) was

added. Periodic monitoring was performed by removing a 200 μL aliquot from the reaction system and diluting it with water by 5 times for fluorescence measurements. Degradation progress was monitored by recording the change in fluorescence intensity of the maximum emission peaks of the UiO-66 derivatives over time. For comparison, degradation progress was also monitored by ^{31}P NMR spectroscopy. To a vial was added UiO-66 derivative (3 mol%) and 10 mL of water and D_2O (9: 1, v/v). After thoroughly mixing, 28 μL of DCP was added under stirring. At a certain interval, a 700 μL aliquot was taken out, and filtered with a 0.22 μm PTFE membrane. The filtrate was collected and transferred to an NMR tube for determining the percent conversion via ^{31}P NMR spectroscopy. Conversion was tracked by measuring decreases in the peaks related to DCP.

Another two simulants, DCNP and DMMP were conducted to validate the generality of the presented methodology. In their degradation experiments, DCNP or DMMP (32 and 21 μL, respectively) was separately added into the aqueous suspension of UiO-66-NH_2 (3 mol%, 10 mL). The following procedures are similar to those described above.

The reusability experiment was studied by taking DCP degradation by UiO-66-NH_2 as an example. Before adding DCP to the aqueous suspension of UiO-66-NH_2, the initial fluorescence intensity (F_0) was recorded. After DCP degradation for 2 h, the fluorescence intensity (F) was measured. The precipitates obtained by centrifuging the above mixture were washed twice with water, and then an appropriate amount of water was added to repeat the above experiment 5 times.

Visual monitoring of degradation of gaseous simulants using UiO-66-NH_2-integrated agarose hydrogels. According to our previous reports,[S3,S4] agarose hydrogels of 2.5% (w/v) were prepared by introducing 0.25 g of agarose to 10 mL of water followed by heating to completely dissolved. Then, 700 μL of UiO-66-NH_2 (1 mg mL^{-1}) was spiked into the above solution and agitated vigorously. After that, 200 μL of the mixture was poured into the inside of cap of the microcentrifuge tube (1.5 mL) and left to be solidified at room temperature.

For visual monitoring of degradation in the vapor phase, a certain volume of

simulants DCP, DCNP, and DMMP (500 μL) were injected into the bottom of the microcentrifuge tube. After closing the cap tightly, the tube was kept upright for a period to produce the simulant vapors and subsequently to permeate into the hydrogels. The color evolution of hydrogels with the exposure time was recorded by a smartphone camera under a UV lamp (365 nm). The relative fluorescence intensity was obtained by analyzing the digital photographs with Image J software.

2. Additional figures and tables

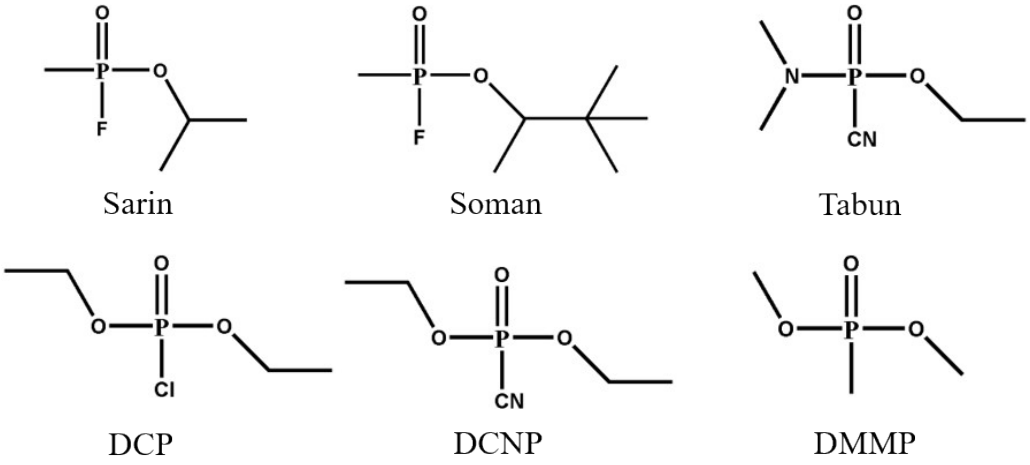

Figure S1. Chemical structures of typical nerve agents and their simulants.

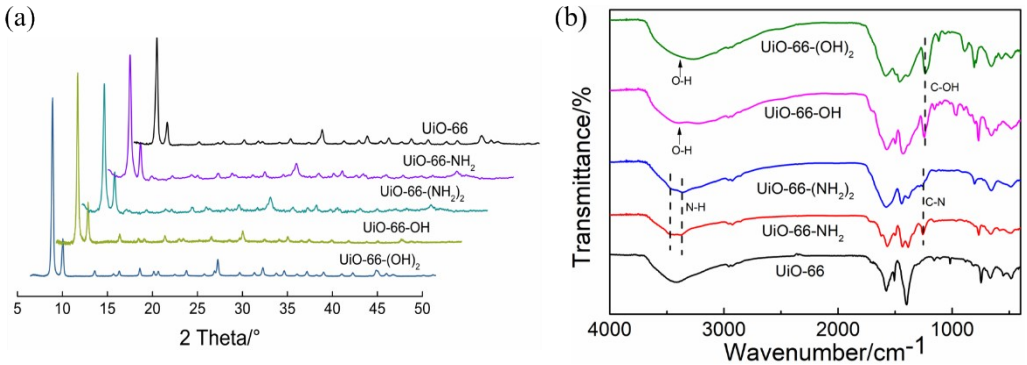

Figure S2. (a) PXRD patterns and (b) FT-IR spectra of UiO-66 and its derivatives.

For UiO-66-NH_2 and UiO-66-$(NH_2)_2$, two absorption peaks at 3000-3500 cm^{-1}, corresponded to the stretching vibration of N-H in amino group, and there is a stretching vibration of C-N at 1257 cm^{-1}. However, there is only one broad O-H stretching vibration at 3000-3500 cm^{-1} and a C-OH stretching band at 1227 cm^{-1} for UiO-66-OH and UiO-66-$(OH)_2$.[S5]

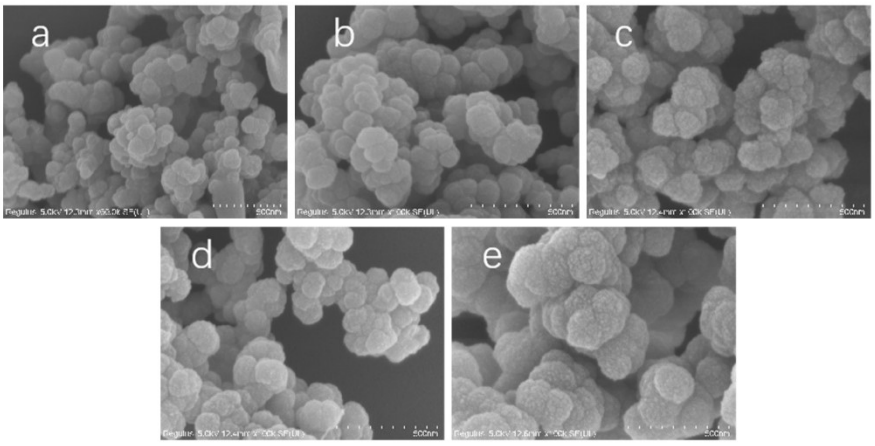

Figure S3. SEM images of (a) UiO-66, (b) UiO-66-NH_2, (c) UiO-66-$(NH_2)_2$, (d) UiO-66-OH and (e) UiO-66-$(OH)_2$.

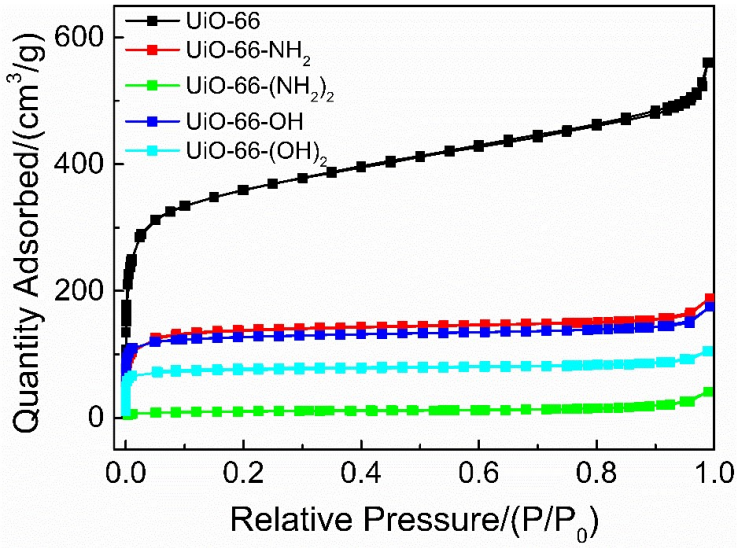

Figure S4. Nitrogen isotherms of UiO-66 and its derivatives at 77 K.

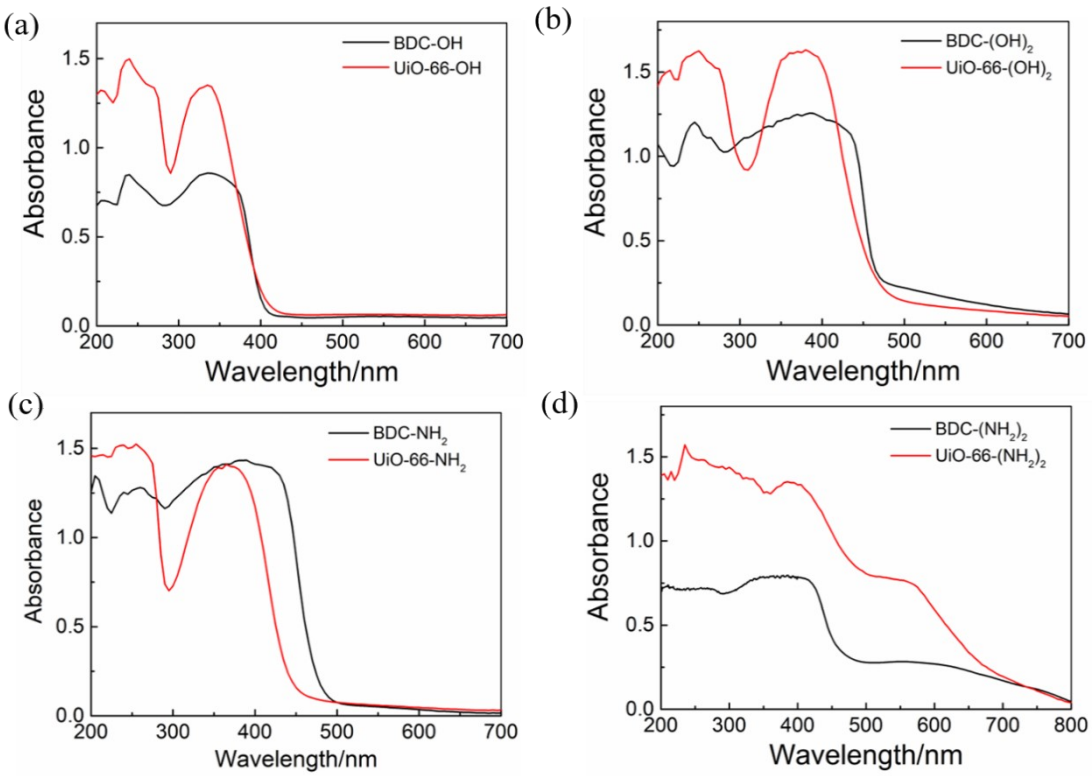

Figure S5. UV-vis diffuse reflectance spectra of four linkers and corresponding MOFs.

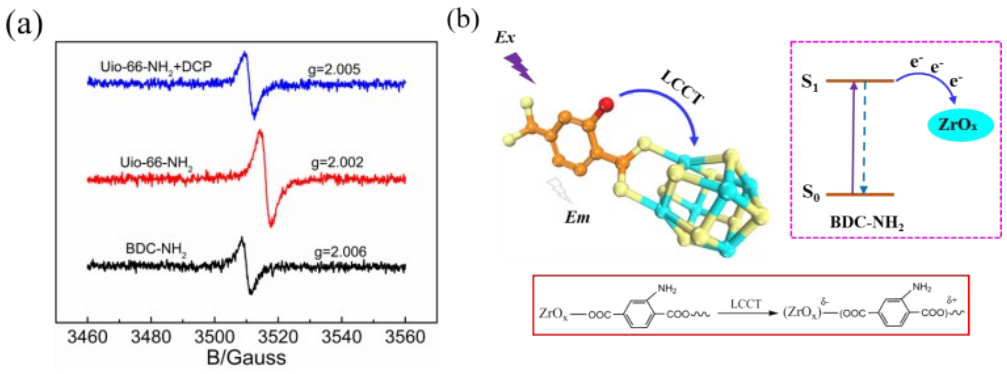

Figure S6. (a) ESR spectra of BDC-NH_2, and UiO-66-NH_2 before and after exposure to DCP in N_2 atmosphere under light irradiation. (b) Schematic illustration of LCCT process in UiO-66-NH_2 and corresponding energy diagram.

Table S1. I_p values of four linkers calculated by CV

Sample	BDC-NH_2	BDC-$(NH_2)_2$	BDC-OH	BDC-$(OH)_2$
I_p/eV	4.97	5.22	5.01	5.16

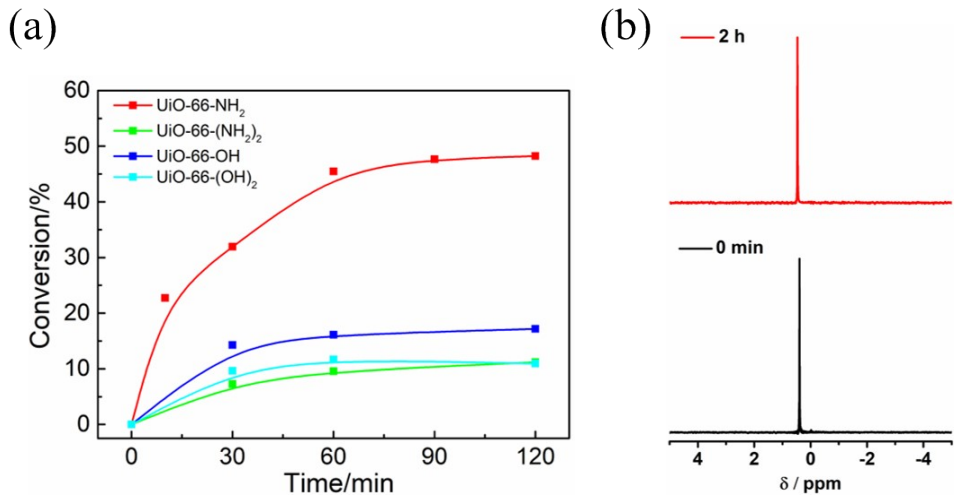

Figure S7. (a) Conversion profiles for degradation of DCP (19 μmol) in the presence of four UiO-66 derivatives as functions of time. (b) ^{31}P NMR spectra showing the hydrolysis of DCP by UiO-66-NH_2 in 0 and 2 h.

It should be noted that in (a) the UiO-66 derivative functionalized by two amino groups on BDC, UiO-66-$(NH_2)_2$, had a very poor activity presumably due to large steric hindrance making DCP very difficult to contact with the active sites.[S6] In (b), the peak at 0.47 ppm assigned to DCP, shifted downfield to 0.55 ppm after catalytic degradation by UiO-66-NH_2, which indicated the formation of the decomposition product, diethyl phosphate.

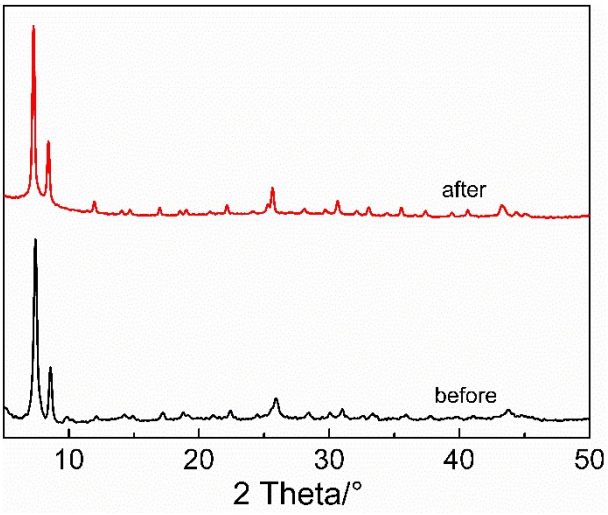

Figure S8. PXRD patterns of UiO-66-NH_2 before and after DCP degradation.

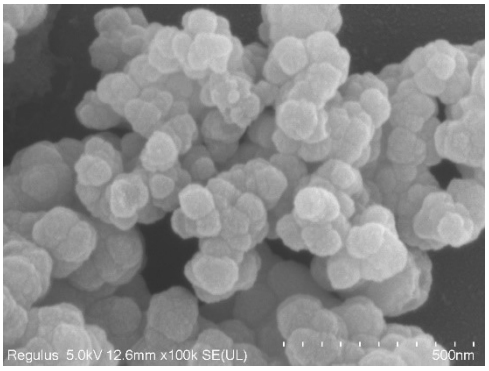

Figure S9. SEM image of UiO-66-NH_2 after DCP degradation.

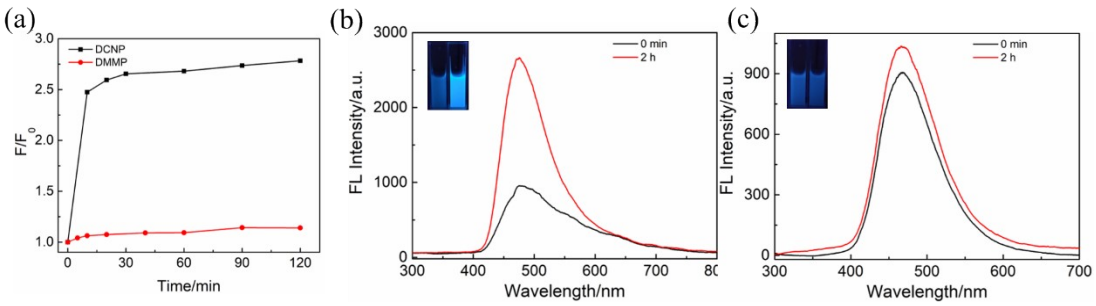

Figure S10. (a) Temporal profiles of the fluorescence intensity ratio (F/F_0) of aqueous suspensions of UiO-66-NH_2 in degradation of DCNP and DMMP (19 μmol). (b) and (c) Corresponding fluorescence spectra of UiO-66-NH_2 for DCNP and DMMP in 0 and 2 h in (a). Inset: corresponding fluorescence photographs in 0 (left) and 2 h (right).

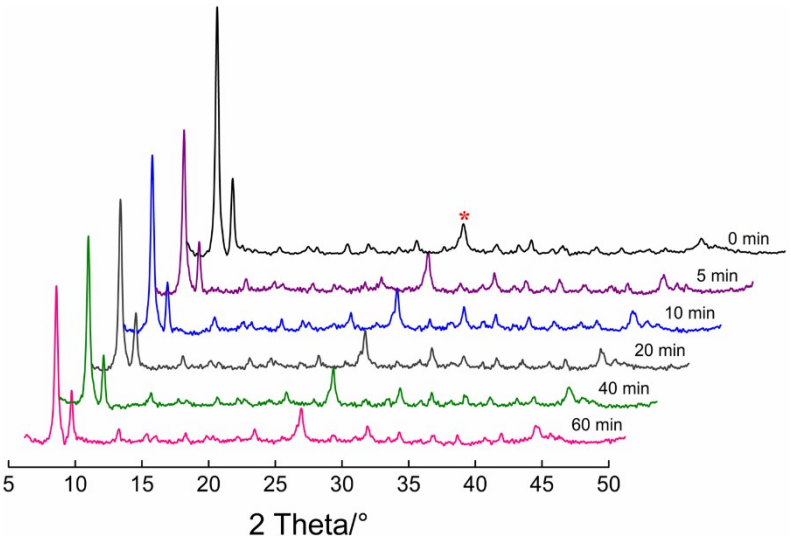

Figure S11. In-situ PXRD of UiO-66-NH_2 during the exposure to DCP. The asterisk denotes high-angle reflections.

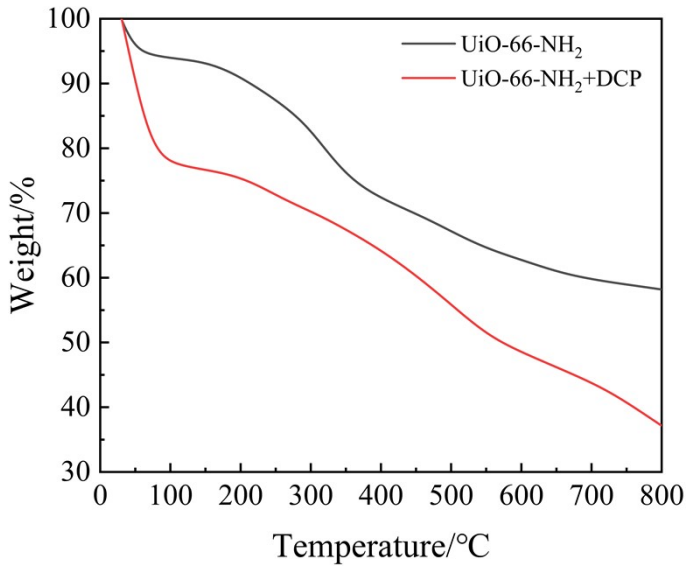

Figure S12. Thermogravimetric analyses of UiO-66-NH_2 before and after exposure to DCP.

The figure showed that a sharp mass loss occurred below 100 °C, which is a result of the removal of DCP adsorbed at the surface. In addition, after exposure to DCP, the mass loss of UiO-66-NH_2 was not so remarkable up to 550 °C compared with the pristine one, suggesting that it became more thermally stable, which could be because that DCP was attached to UiO-66-NH_2 via strong binding between P=O functional group and Zr-oxo clusters.

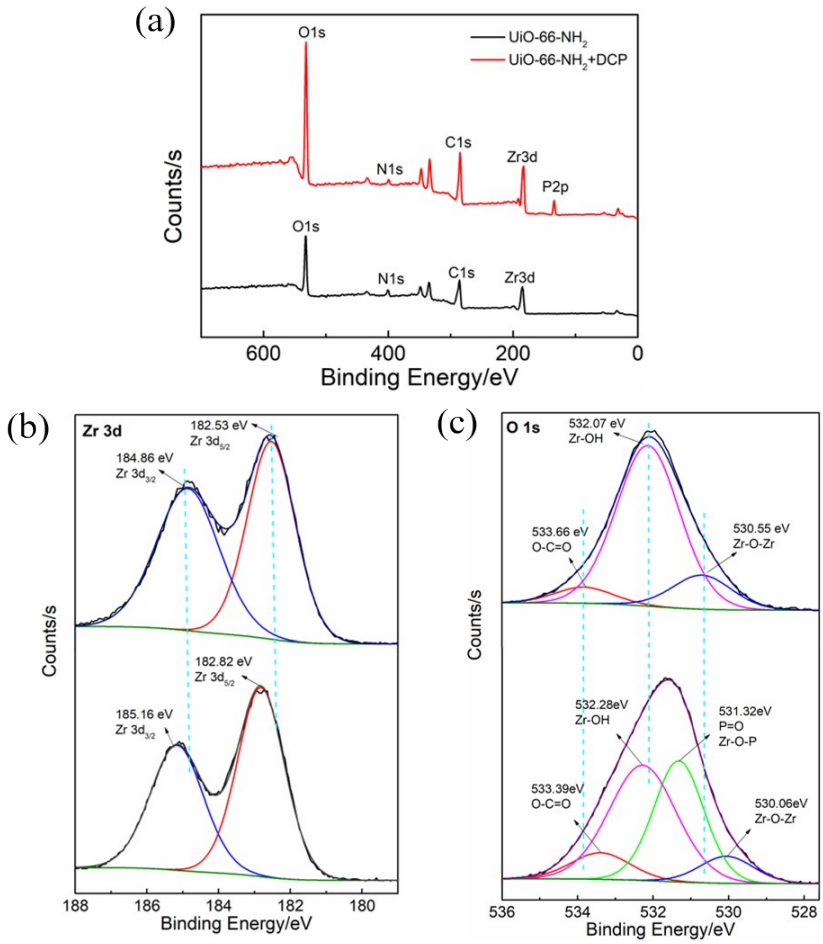

Figure S13. (a) Full-scale XPS spectra of UiO-66-NH_2 before and after exposure to DCP. High-resolution XPS spectra of Zr 3d (b) and O 1s (c) before (top) and after (bottom) exposure to DCP.

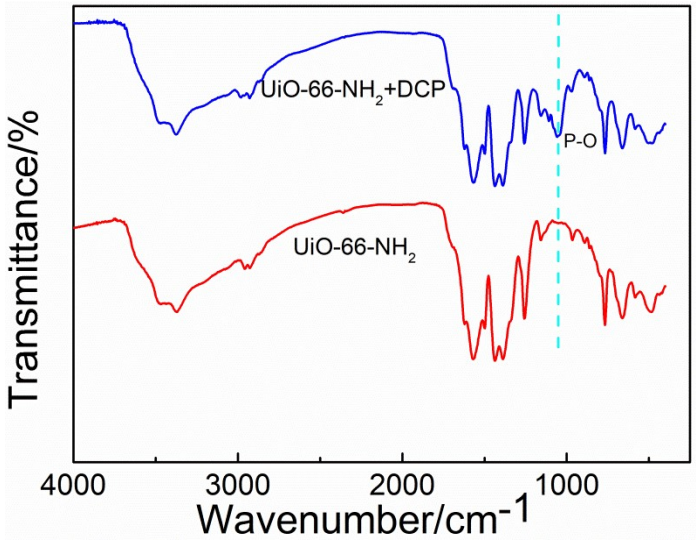

Figure S14. FT-IR of UiO-66-NH_2 before and after exposure to DCP.

For UiO-66-NH_2, three strong absorption peaks at 1568, 1436, and 1387 cm^{-1} originate from the carboxyl group of BDC-NH_2. The triplet peaks in 500-800 cm^{-1} stem from O-Zr-O as longitudinal and transverse modes.[S7] After DCP degradation, a new absorption peak appeared at 1058 cm^{-1}, which corresponds to the asymmetrical stretching vibration of P-O bonds, indicating that hydrolysis product of DCP were successfully anchored onto UiO-66-NH_2.

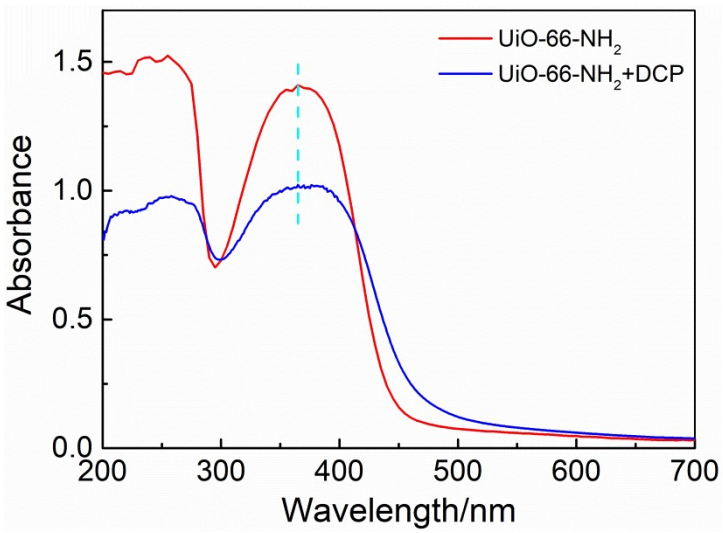

Figure S15. UV-vis diffuse reflectance spectra of UiO-66-NH_2 before and after exposure to DCP.

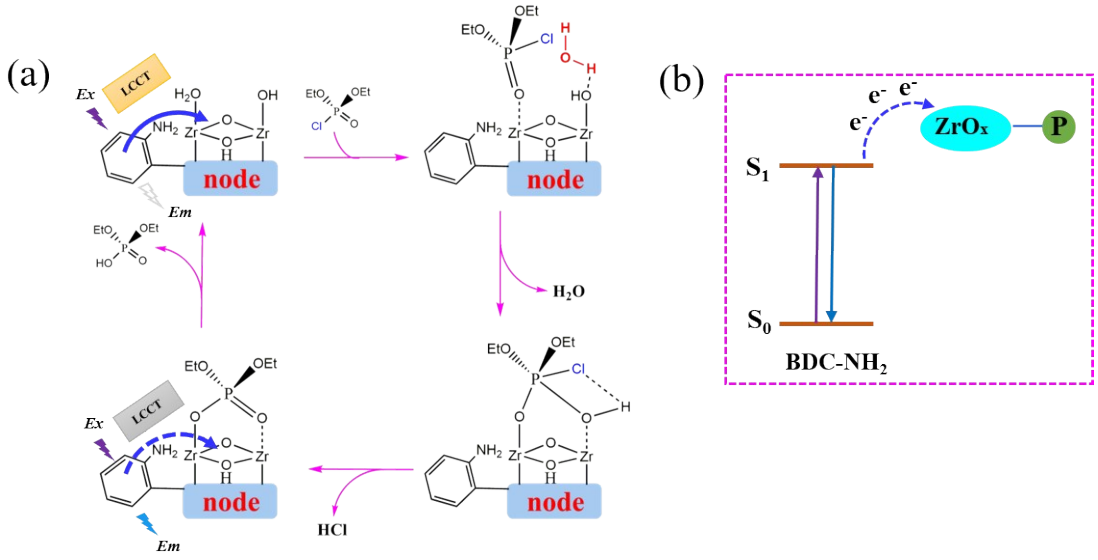

Scheme S1. (a) Schematic illustration of proposed DCP degradation mechanism by UiO-66-NH_2 and change in LCCT process. (b) Corresponding

energy diagram.

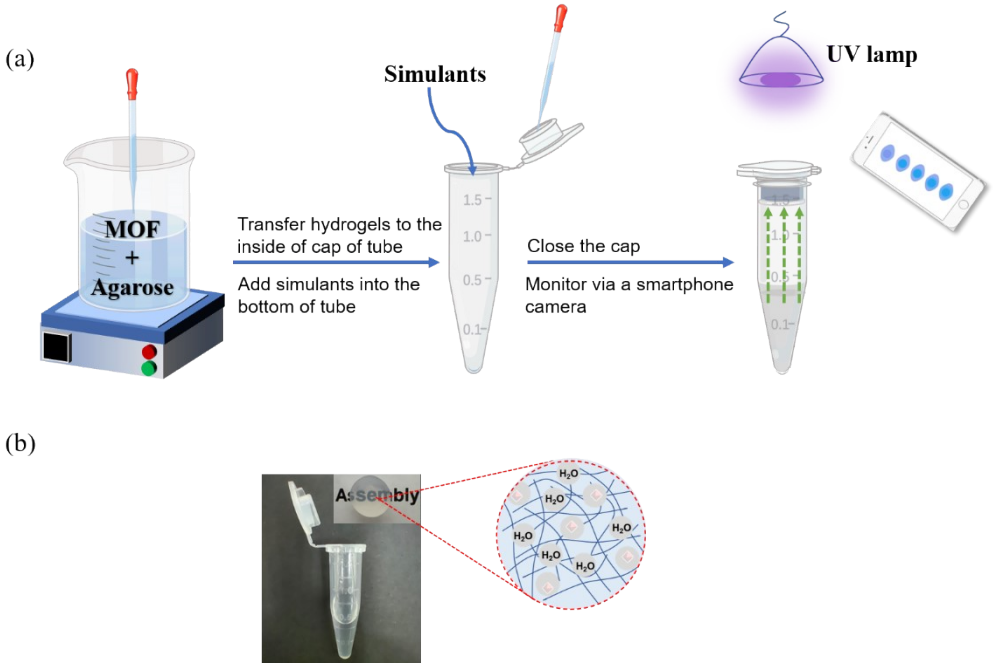

Figure S16. (a) Schematic of the protocol for visual monitoring of simulant vapors by UiO-66-NH_2-integrated agarose hydrogels using an "olfactory system" constructed by an enclosed microcentrifuge tube. (b) Corresponding photographs and proposed composition sketch where the octahedron represents UiO-66-NH_2.

In this system, the hybrid hydrogels adhered to the inside of cap of the tube, and the simulants stood at the bottom of the tube. As the simulants gradually evaporated, the produced vapors can permeate into the network of the hybrid hydrogels, and be subsequently catalytically degraded by the entrapped UiO-66-NH_2. Accordingly, the quenched fluorescence of UiO-66-NH_2 was switched on and gradually enhanced under UV irradiation.

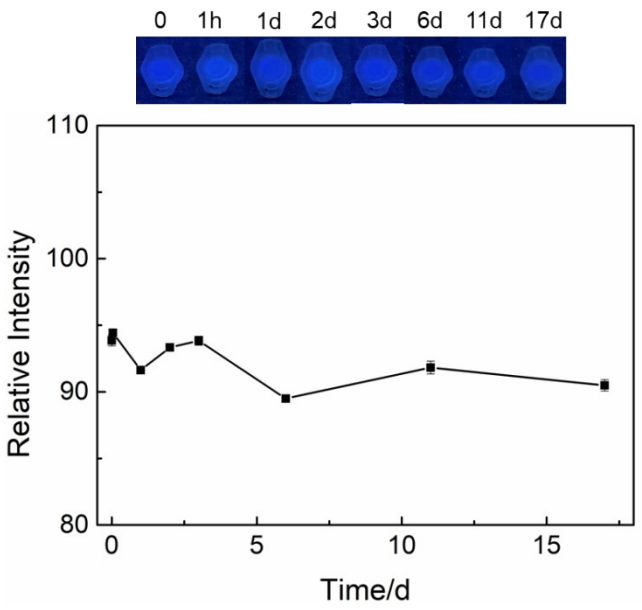

Figure S17. Temporal profiles of the relative fluorescence intensity of UiO-66-NH_2-integrated agarose hydrogels determined from the digital photographs (upper inset) by Image J.

3. References

(S1) Li, Y. C.; Zhong, H. Z.; Li, R.; Zhou, Y.; Yang, C. H.; Li, Y. F. *Adv. Funct. Mater.* **2006**, *16*, 1705-1716.

(S2) Katz, M. J.; Brown, Z. J.; Colon, Y. J.; Siu, P. W.; Scheidt, K. A.; Snurr, R. Q.; Hupp, J. T.; Farha, O. K. *Chem. Commun.* **2013**, *49*, 9449-9451.

(S3) Rada, Z. H.; Abid, H. R.; Shang, J.; Sun, H.; He, Y.; Webley, P.; Liu, S.; Wang, S. *Ind. Eng. Chem. Res.* **2016**, *55*, 7924-7932.

(S4) Gao, N.; Huang, J.; Wang, L.; Feng, J.; Huang, P.; Wu, F. *Appl. Surf. Sci.* **2018**, *459*, 686-692.

(S5) Huang, P.; Liu, Y.; Karmakar, A.; Yang, Q.; Li, J.; Wu, F. Y.; Deng, K. Y. *Dalton Trans.* **2021**, *50*, 6901-6912.

(S6) Katz, M. J.; Moon, S. Y.; Mondloch, J. E.; Beyzavi, M. H.; Stephenson, C. J.; Hupp, J. T.; Farha, O. K. *Chem. Sci.* **2015**, *6*, 2286-2291.

(S7) Cavka, J. H.; Jakobsen, S.; Olsbye, U.; Guillou, N.; Lamberti, C.; Bordiga, S.; Lillerud, K. P. *J. Am. Chem. Soc.* **2008**, *130*, 13850-13851.